

# Product Distributions from the OH Radical-Induced Oxidation of *n*-Pentane and Isopentane (2-Methylbutane) in Air

GERALD HEIMANN, PETER WARNECK

Max-Planck-Institut für Chemie, 55020 Mainz, Germany

Received 18 October 2005; revised 5 May 2006; accepted 13 May 2006

DOI 10.1002/kin.20200

Published online in Wiley InterScience (www.interscience.wiley.com).

**ABSTRACT:** Hydroxyl radicals, generated by photolysis of H<sub>2</sub>O<sub>2</sub>, were reacted with *n*-pentane and isopentane in air in the absence of nitrogen oxides. The observed product distributions were compared with similar data derived by computer simulations, based on the known reaction mechanisms, to determine relative probabilities for hydrogen abstraction at different sites of the parent compounds and to estimate branching ratios and relative rate coefficients for cross-combination reactions between different peroxy radicals. For *n*-pentane, the distribution of the pentanols indicates probabilities for hydrogen abstraction, in percent, of  $q_1 = 9.1 \pm 0.7$ ,  $q_2 = 56.1 \pm 1.8$ , and  $q_3 = 34.8 \pm 1.3$ , which agree with predictions based on the algorithm proposed by Atkinson. Branching ratios needed to harmonize calculated and observed product distributions are somewhat larger than, although still within the error ranges of, the values found by us previously. Comparison between experimental and calculated data confirms the isomerization and decomposition constants recently established for the three pentoxyl radical isomers. The product distribution for isopentane, which is dominated by acetone, acetaldehyde, 2-methyl-butan-2-ol, and 2-methyl-butan-2-hydroperoxide, is in harmony with the predicted oxidation mechanism. Probabilities for hydrogen abstraction from isopentane were estimated to occur to 12% at the primary, 28% at the secondary, and 60% at the tertiary sites, again in agreement with predictions based on the algorithm of Atkinson. © 2006 Wiley Periodicals, Inc. *Int J Chem Kinet* 38: 677–688, 2006

---

Correspondence to: Peter Warneck; e-mail: Peter.Warneck@gmx.de.

Contract grant sponsor: German Federal Ministry for Research and Technology.

© 2006 Wiley Periodicals, Inc.

## INTRODUCTION

Pentanes are components of automotive fuels that enter the atmosphere by fuel evaporation and with the engine exhaust gases. As for other alkanes, the dominant loss process in the troposphere is reaction with the hydroxyl radical. This initiates an oxidation process leading to aldehydes and ketones, with alkylperoxy and alkoxy radicals acting as intermediates [1–3]. The detailed reaction pathways are of interest not only to atmospheric chemistry but also to a better understanding of low-temperature oxidation of alkanes in general. Reaction mechanisms for the pentanes have remained somewhat speculative, because hydrogen abstraction may occur at different sites of the molecule and the subsequent addition of O<sub>2</sub> generates several isomeric pentylperoxy radicals, three in the case of *n*-pentane and four in the case of isopentane. Probabilities for their formation can be estimated using formulas developed by Greiner [4] and Atkinson [5,6] for the abstraction of a primary, secondary, or tertiary hydrogen atom from the alkane. In urban and suburban atmospheres, where nitrogen oxides are abundant, pentylperoxy radicals are largely converted to pentoxyl radicals by reacting with NO. Pentoxyl radicals, in turn, react partly with oxygen to form carbonyl compounds, and they undergo isomerization and/or decomposition, thereby generating new alkylperoxy radicals. Although these processes have received much attention, the rate coefficients associated with reactions of *n*-pentoxyl isomers have been determined with some reliability only recently, experimentally [7–10] as well as theoretically [11–14]. In the absence of NO, the pentylperoxy radicals react with each other and with other alkylperoxy radicals generated in the system; one branch of each reaction leads again to pentoxyl radicals, the other to alcohols and carbonyl compounds. Table I summarizes the principal reactions occurring in the oxidation of *n*-pentane.

We have previously studied the reaction sequences following the self-reactions of individual *n*-pentylperoxy radicals formed by photolysis of the corresponding iodopentanes [9]. Here, we present results for the OH-induced oxidation of *n*-pentane, carried out under similar NO<sub>x</sub>-free conditions. The system involves the mutual interactions of the 7 peroxy radicals characterized in Fig. 1. In addition, we have explored the oxidation of isopentane and present our results below. An effort was made to determine the full product spectrum in each case. This has not been attempted previously, to our knowledge. Computer simulations were carried out to assist in the data analysis; for *n*-pentane, the previous data were utilized as far as possible. Product distributions provide information on the probability

of hydrogen abstraction at the different reaction sites and on the branching ratios of some cross-combination reactions compared to the self-reactions of peroxy radicals.

## EXPERIMENTAL TECHNIQUES

Apparatus and experimental procedures were similar to those described previously [15]. The reactions were carried out in 2-L spherical glass bulbs. Hydroxyl radicals were generated by photolysis of hydrogen peroxide using 254 nm radiation derived from an ozone-free penray mercury lamp, which was placed into a quartz finger reaching into the center of the bulb. The lamp was cooled by a flow of compressed nitrogen. The bulbs were fitted with Teflon-stoppered shutoff valves and joints for connection to a gas-handling manifold. Reaction mixtures consisted of approximately 120 ppm H<sub>2</sub>O<sub>2</sub> and 0.1% hydrocarbon (mole fraction) in synthetic air at a pressure slightly above atmospheric. The H<sub>2</sub>O<sub>2</sub> mixing ratio was determined by the vapor pressure above a concentrated aqueous solution of H<sub>2</sub>O<sub>2</sub> kept in an ice bath. The actual mixing ratio depended on the extent of equilibration, so that it was sometimes lower than 120 ppm. In some experiments, when a higher product yield was desirable, the ice bath was removed to allow the vapor pressure to rise. The estimated range of H<sub>2</sub>O<sub>2</sub> mixing ratios was 70–350 ppm.

Product concentrations were determined by gas chromatography with flame ionization detectors. Samples of the reaction mixtures were transferred to the gas chromatograph via thin Teflon tubes pushed through a hole pierced in a septum attached to the reaction vessel. Two septa and transfer lines were needed when the analysis required the simultaneous application of two GC systems. Inlet lines and sampling loops of the gas chromatographs were made of quartz-lined stainless steel tubes. The sampling valve was kept at a temperature of 80°C. Two capillary columns (50 m long, 0.32 mm i.d.) were required to separate the products: a CPSil 76 column, coated with dimethylpolysiloxane (0.34 μm film thickness); and a CP-Wax 57 CB column, coated with polyethylene glycol (0.23 μm film thickness). The nitrogen carrier flow rate was 3 cm<sup>3</sup> min<sup>-1</sup> for both. The temperature programs also were similar: 30°C isothermal for 3 min, heating to 65°C at a rate of 8°C min<sup>-1</sup>, followed by further heating to 200°C at a rate of 30°C min<sup>-1</sup>, and finally constant for 3 min at 200°C. In some experiments, the CP-Wax 57 column was replaced by a CP-Wax 52 column with the following temperature program: 40°C isothermal for 2 min, heating to 160°C at a rate of 20°C min<sup>-1</sup>, followed

**Table I** Reactions of Pentylperoxy Radicals and the Resulting Products<sup>a</sup>

|   |  |                                      |
|---|--|--------------------------------------|
| $\text{OH} + n\text{-C}_5\text{H}_{12} (+\text{O}_2)$   | $\rightarrow \text{C}_4\text{H}_9\text{CH}_2\text{OO}\cdot + \text{H}_2\text{O}$   | $q_1 k_{\text{OH}}$                  |
|   | $\rightarrow \text{CH}_3\text{CH}(\text{OO}\cdot)\text{C}_3\text{H}_7 + \text{H}_2\text{O}$  | $q_2 k_{\text{OH}}$                  |
|   | $\rightarrow \text{C}_2\text{H}_5\text{CH}(\text{OO}\cdot)\text{C}_2\text{H}_5 + \text{H}_2\text{O}$   | $q_3 k_{\text{OH}}$                  |
| $\text{C}_4\text{H}_9\text{CH}_2\text{OO}\cdot + \text{R}_1\text{CH}(\text{OO}\cdot)\text{R}_2$                           | $\rightarrow \text{C}_4\text{H}_9\text{CH}_2\text{O}\cdot + \text{R}_1\text{CH}(\text{O}\cdot)\text{R}_2$  | $\alpha_{11} k_{11}$                 |
|   | $\rightarrow \text{C}_4\text{H}_9\text{CHO} + \text{R}_1\text{CH}(\text{OH})\text{R}_2$  | $\gamma_{11}(1 - \alpha_{11})k_{11}$ |
|   | $\rightarrow \text{C}_4\text{H}_9\text{CH}_2\text{OH} + \text{R}_1\text{COR}_2$  | $z_{11}(1 - \alpha_{11})k_{11}$      |
|   | $\rightarrow \text{C}_4\text{H}_9\text{CHO} + \text{HO}_2$   | $p k_{\text{O}_2}$                   |
| $\text{C}_4\text{H}_9\text{CH}_2\text{O}\cdot + \text{O}_2$   | $\rightarrow \text{CH}_3\text{CH}(\text{OO}\cdot)(\text{CH}_2)_2\text{CH}_2\text{OH}$  | $^1 k_{\text{isom}}$                 |
| $\text{C}_4\text{H}_9\text{CH}_2\text{O}\cdot (+\text{O}_2)$  | $\rightarrow \text{CH}_3\text{CH}(\text{O}\cdot)(\text{CH}_2)_2\text{CH}_2\text{OH} + \text{R}_1\text{CH}(\text{O}\cdot)\text{R}_2 + \text{O}_2$ | $\alpha_{61} k_{61}$                 |
| $\text{CH}_3\text{CH}(\text{OO}\cdot)(\text{CH}_2)_2\text{CH}_2\text{OH} + \text{R}_1\text{CH}(\text{OO}\cdot)\text{R}_2$ | $\rightarrow \text{CH}_3\text{CO}(\text{CH}_2)_2\text{CH}_2\text{OH} + \text{R}_1\text{CHOHR}_2 + \text{O}_2$                                    | $\gamma_{61}(1 - \alpha_{61})k_{61}$ |
|   | $\rightarrow \text{CH}_3\text{CHO}(\text{CH}_2)_2\text{CH}_2\text{OH} + \text{R}_1\text{COR}_2 + \text{O}_2$                                     | $z_{61}(1 - \alpha_{61})k_{61}$      |
| $\text{CH}_3\text{CH}(\text{O}\cdot)(\text{CH}_2)_2\text{CH}_2\text{OH}$  | $\rightarrow \text{CH}_3\text{CHOH}(\text{CH}_2)_2\text{CH}_2\text{O}\cdot$  | $^6 k_{\text{isom}}$                 |
| $\text{CH}_3\text{CHOH}(\text{CH}_2)_2\text{CH}_2\text{O}\cdot + \text{O}_2$  | $\rightarrow \text{CH}_3\text{CHOH}(\text{CH}_2)_2\text{CHO} + \text{HO}_2$  | $p k_{\text{O}_2}$                   |
| $\text{CH}_3\text{CH}(\text{OO}\cdot)\text{C}_3\text{H}_7 + \text{R}_1\text{CH}(\text{OO}\cdot)\text{R}_2$                | $\rightarrow \text{CH}_3\text{CH}(\text{O}\cdot)\text{C}_3\text{H}_7 + \text{R}_1\text{CH}(\text{O}\cdot)\text{R}_2 + \text{O}_2$                | $\alpha_{21} k_{21}$                 |
|   | $\rightarrow \text{CH}_3\text{COC}_3\text{H}_7 + \text{R}_1\text{CHOHR}_2 + \text{O}_2$  | $\gamma_{21}(1 - \alpha_{21})k_{21}$ |
|   | $\rightarrow \text{CH}_3\text{CHOHC}_3\text{H}_7 + \text{R}_1\text{COR}_2 + \text{O}_2$  | $z_{21}(1 - \alpha_{21})k_{21}$      |
| $\text{CH}_3\text{CH}(\text{O}\cdot)\text{C}_3\text{H}_7 + \text{O}_2$  | $\rightarrow \text{CH}_3\text{COC}_3\text{H}_7 + \text{HO}_2$  | $^s k_{\text{O}_2}$                  |
| $\text{CH}_3\text{CH}(\text{O}\cdot)\text{C}_3\text{H}_7 (+\text{O}_2)$   | $\rightarrow \text{CH}_3\text{CHO} + \text{C}_3\text{H}_7\text{OO}\cdot$   | $^2 k_{\text{dec}}$                  |
| $\text{CH}_3\text{CH}(\text{O}\cdot)\text{C}_3\text{H}_7 (+\text{O}_2)$   | $\rightarrow \text{CH}_3\text{CHOH}(\text{CH}_2)_2\text{CH}_2\text{OO}\cdot$   | $^2 k_{\text{isom}}$                 |
| $\text{CH}_3\text{CHOH}(\text{CH}_2)_2\text{CH}_2\text{OO}\cdot + \text{R}_1\text{CH}(\text{OO}\cdot)\text{R}_2$          | $\rightarrow \text{CH}_3\text{CHOH}(\text{CH}_2)_2\text{CH}_2\text{O}\cdot + \text{R}_1\text{CH}(\text{O}\cdot)\text{R}_2 + \text{O}_2$          | $\alpha_{71} k_{71}$                 |
|   | $\rightarrow \text{CH}_3\text{CHOH}(\text{CH}_2)_2\text{CH}_2\text{OH} + \text{R}_1\text{CHOHR}_2 + \text{O}_2$                                  | $\gamma_{71}(1 - \alpha_{71})k_{71}$ |
|   | $\rightarrow \text{CH}_3\text{CHOH}(\text{CH}_2)_2\text{CH}_2\text{OH} + \text{R}_1\text{COR}_2 + \text{O}_2$                                    | $z_{71}(1 - \alpha_{71})k_{71}$      |
| $\text{CH}_3\text{CHOH}(\text{CH}_2)_2\text{CH}_2\text{O}\cdot + \text{O}_2$  | $\rightarrow \text{CH}_3\text{CHOH}(\text{CH}_2)_2\text{CHO} + \text{HO}_2$  | $p k_{\text{O}_2}$                   |
| $\text{CH}_3\text{CHOH}(\text{CH}_2)_2\text{CH}_2\text{O}\cdot$   | $\rightarrow \text{CH}_3\text{CH}(\text{O}\cdot)(\text{CH}_2)_2\text{CH}_2\text{OH}$   | $^7 k_{\text{isom}}$                 |
| $\text{CH}_3\text{CH}(\text{O}\cdot)(\text{CH}_2)_2\text{CH}_2\text{OH} + \text{O}_2$                                     | $\rightarrow \text{CH}_3\text{CO}(\text{CH}_2)_2\text{CH}_2\text{OH} + \text{HO}_2$  | $^s k_{\text{O}_2}$                  |
| $\text{CH}_3\text{CH}(\text{O}\cdot)(\text{CH}_2)_2\text{CH}_2\text{OH} + \text{O}_2$                                     | $\rightarrow \text{C}_2\text{H}_5\text{CH}(\text{O}\cdot)\text{C}_2\text{H}_5 + \text{R}_1\text{CH}(\text{O}\cdot)\text{R}_2 + \text{O}_2$       | $\alpha_{31} k_{31}$                 |
| $\text{C}_2\text{H}_5\text{CH}(\text{OO}\cdot)\text{C}_2\text{H}_5 + \text{R}_1\text{CH}(\text{OO}\cdot)\text{R}_2$       | $\rightarrow \text{C}_2\text{H}_5\text{COC}_2\text{H}_5 + \text{R}_1\text{CHOHR}_2 + \text{O}_2$   | $\gamma_{31}(1 - \alpha_{31})k_{31}$ |
|   | $\rightarrow \text{C}_2\text{H}_5\text{CHOHC}_2\text{H}_5 + \text{R}_1\text{COR}_2 + \text{O}_2$   | $z_{31}(1 - \alpha_{31})k_{31}$      |
| $\text{C}_2\text{H}_5\text{CH}(\text{O}\cdot)\text{C}_2\text{H}_5 + \text{O}_2$   | $\rightarrow \text{C}_2\text{H}_5\text{COC}_2\text{H}_5 + \text{HO}_2$   | $^s k_{\text{O}_2}$                  |
| $\text{C}_2\text{H}_5\text{CH}(\text{O}\cdot)\text{C}_2\text{H}_5 (+\text{O}_2)$  | $\rightarrow \text{C}_2\text{H}_5\text{CHO} + \text{C}_2\text{H}_5\text{OO}\cdot$  | $^3 k_{\text{dec}}$                  |
| $\text{HO}_2 + \text{R}_1\text{CH}(\text{OO}\cdot)\text{R}_2$   | $\rightarrow \text{R}_1\text{CH}(\text{OOH})\text{R}_2 + \text{O}_2$   | $k_{\text{HO}_2}$                    |
| $\text{HO}_2 + \text{HO}_2$   | $\rightarrow \text{H}_2\text{O}_2 + \text{O}_2$  | $k_{\text{H}_2\text{O}_2}$           |

<sup>a</sup>  $\text{R}_1\text{CH}(\text{OO}\cdot)\text{R}_2$  represents one of the peroxy radicals in Fig. 1; subscripts of rate coefficients and branching ratios ( $i = 1-7$ ) correspond to the numbering of radicals in the figure.

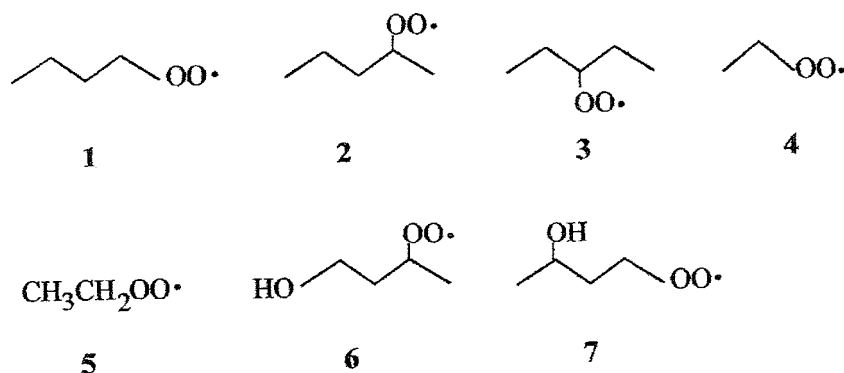


**Figure 1** Peroxyl radicals occurring in the oxidation of *n*-pentane and their identification by numbers. The numbers are used as subscripts of rate coefficients and branching ratios associated with mutual reactions.

by further heating to 210°C at a rate of 30°C min<sup>-1</sup>, and finally constant for 3 min at 210°C. Products were identified by comparison of retention times with authentic samples of alcohols, aldehydes, and ketones. Calibration curves for peak area versus concentration of individual compounds were obtained with samples prepared by successive dilution of mixtures containing known amounts of the pure substance in air. Daily calibration checks were then carried out with suitable mixtures of substances in air that covered the concentration range encountered. Most of the substances were available commercially with a purity of at least 99.9%. In the oxidation of *n*-pentane, the CPSil column showed a product eluting after 9.9 min retention time, about 3 min later than the main group of alcohols and carbonyl compounds. Because this is typical of a bifunctional compound, the additional peak was assigned to be an isomerization product. In this case, 4-hydroxy-3-methylbutan-2-one was used as a surrogate for calibration because its retention time was close to that of the unknown product. Subsequent to completing the bulk of the experiments, one of the expected isomerization products, 1-hydroxy-pentan-4-one, became commercially available. Both compounds were compared on the CP-Wax 52 column. Their response was similar but the latter eluted much later than the former. The

present study was not focused on isomerization products, and no attempts were made to identify them.

## MODEL CALCULATIONS

The FACSIMILE computer code [16] was employed to calculate the rise of product concentrations with time and the ensuing product distributions. Calculations were based on comprehensive chemical mechanisms that took into account the interactions of all peroxy radicals in the system as well as reactions of the alkoxy radicals. These reactions were added to the basic reactions involving H<sub>2</sub>O<sub>2</sub> and HO<sub>2</sub> radicals. Rate coefficients applied for the reactions of OH radicals with *n*-pentane and isopentane are 4.0 × 10<sup>-12</sup> and 3.7 × 10<sup>-12</sup> cm<sup>3</sup> molecule<sup>-1</sup> s<sup>-1</sup>, respectively [1]. More recent values presented by Atkinson and Arey [2] are slightly lower: 3.8 × 10<sup>-12</sup> and 3.6 × 10<sup>-12</sup> cm<sup>3</sup> molecule<sup>-1</sup> s<sup>-1</sup>, but using these data would have no effect on the relative product distributions. Relative probabilities for hydrogen abstraction at different sites of the two alkanes were initially estimated from the experimental data and subsequently refined by the calculations. Table I shows the principal reactions occurring during the oxidation of *n*-pentane, Table II summarizes

**Table II** Known Rate Coefficients and Branching Ratios (at 298 K) Involved in *n*-Pentane Oxidation

|  |
|--|
| $k(\text{OH} + n\text{-pentane}) = 4.0 \times 10^{-12} \text{ cm}^3 \text{ molecule}^{-1} \text{ s}^{-1}$ [1]  |
| $\alpha_{11} = 0.42 \pm 0.17, \alpha_{22} = 0.46 \pm 0.10, \alpha_{33} = 0.40 \pm 0.08$ [9]  |
| $k_{44} = 3.0 \times 10^{-13} \text{ cm}^3 \text{ molecule}^{-1} \text{ s}^{-1}$ [1,17]  |
| $k_{55} = (6.6 \pm 0.2) \times 10^{-14} \text{ cm}^3 \text{ molecule}^{-1} \text{ s}^{-1}, \alpha_{55} = 0.63 \pm 0.06$ [1,17]   |
| $^1k_{\text{isom}} = (4.0 \pm 1.1) \times 10^5 \text{ s}^{-1}$ [9], $2.0 \times 10^6 \text{ s}^{-1}$ [12], $2.2 \times 10^6 \text{ s}^{-1}$ [14]   |
| $^2k_{\text{isom}} = 2.5 \times 10^5 \text{ s}^{-1}$ [7,11], $(1.0 \pm 0.2) \times 10^5 \text{ s}^{-1}$ [9], $5.0 \times 10^5 \text{ s}^{-1}$ [12], $3.3 \times 10^5 \text{ s}^{-1}$ [14]  |
| $^2k_{\text{dec}} = 9.1 \times 10^3 \text{ s}^{-1}$ [7,11], $(8.4 \pm 1.7) \times 10^3 \text{ s}^{-1}$ [9], $1.0 \times 10^4 \text{ s}^{-1}$ [12], $2.2 \times 10^4 \text{ s}^{-1}$ [13]   |
| $^3k_{\text{dec}} = 2.6 \times 10^4 \text{ s}^{-1}$ [8,11], $(2.6 \pm 0.3) \times 10^4 \text{ s}^{-1}$ [9], $(3.3 \pm 0.65) \times 10^4 \text{ s}^{-1}$ [10], $3.3 \times 10^4 \text{ s}^{-1}$ [12], $3.4 \times 10^4 \text{ s}^{-1}$ [13] |

known values of rate coefficients and branching ratios for this system, and Fig. 1 shows structures of the peroxy radicals involved in the oxidation of *n*-pentane and the number code used to identify their interactions by suffixes of rate coefficients and branching ratios. Major uncertainties exist for the rate coefficients of peroxy radicals, mainly C5 alkyl peroxy and hydroxy-alkyl peroxy radicals, because most of them have not been measured. Accordingly, we had to work with estimates. As previously [9,15], we have differentiated between primary, secondary, and tertiary alkylperoxy radicals and applied for their self-reactions values of  $2 \times 10^{-13}$ ,  $2 \times 10^{-15}$ , and  $2.5 \times 10^{-17}$  cm<sup>3</sup> molecule<sup>-1</sup> s<sup>-1</sup>, respectively, corresponding to known rate coefficients for other alkylperoxy radical self-reactions [1,17]. Rate constants for cross-combination reactions of different types of peroxy radicals were initially derived by taking the root over the product of the values for the self-reactions [18]. Changes were made only if they led to a better agreement with the observed product distributions. The branching ratios for cross-combination reactions also are uncertain. For primary and secondary alkylperoxy radicals, we have initially used branching ratios  $\alpha_{ki} = 0.5$  for the radical preserving channel and  $0.5(1 - \alpha_{ki})$  for each channel leading to alcohols and carbonyl compounds. Adjustments were made only if necessary to achieve to a better simulation of the observed product distribution. The reaction site of tertiary peroxy radicals lacks the hydrogen atom that must be transferred to form a primary or secondary alcohol so that in the interaction with primary or secondary peroxy radicals only two reaction channels exist. In these cases, the branching ratios  $\alpha_{ki} = 0.4$  and  $(1 - \alpha_{ki}) = 0.6$  were applied in accordance with previous results [15]. The rate coefficients and branching ratios for the self-reactions of ethyl peroxy and propyl peroxy radicals are known [1,17], and the appropriate values were employed. Reactions of alkoxy radicals with oxygen were assigned rate coefficients suggested by Atkinson [1]:  ${}^p k_{O_2} = 9.5 \times 10^{-15}$  for primary alkoxy, and  ${}^s k_{O_2} = 8.0 \times 10^{-15}$  cm<sup>3</sup> molecule<sup>-1</sup> s<sup>-1</sup> for secondary alkoxy radicals. Reactions between alkoxy and alkylperoxy radicals can be neglected. The concentrations of peroxy radicals are not high enough for such reactions to compete with the other reactions of alkoxy radicals (with oxygen, decomposition, isomerization), even if very large rate coefficients were applicable. Reactions of HO<sub>2</sub> with alkyl peroxy radicals lead to the formation of hydroperoxides. They were assigned rate coefficients  $k_{HO_2} = 1.5 \times 10^{-11}$  cm<sup>3</sup> molecule<sup>-1</sup> s<sup>-1</sup> for C5 peroxy radicals. The rate coefficient for HO<sub>2</sub> with ethyl peroxy is known [1,17]. Further details will be given in the Results section.

## RESULTS

### *n*-Pentane

The following products were detected and quantified: ethanal, propanal, pentanal, and the two isomeric pentanones, the three pentanols, and one or more unspecified isomerization products, occurring on the CPSil column at a retention time typical of a C5 hydroxy-carbonyl compound. Small amounts of ethanol and propan-1-ol were also detected. Butanal, which was observed in the photo-oxidation of 1-iodopentane, could not be unambiguously identified. Two GC columns were required to separate the products. The CPSil 76 column separated pentanal and the two pentanones but not the pentanols, whereas the CP-Wax columns separated the pentanols but not the C5 carbonyl compounds. The distributions of carbonyl compounds and alcohols were measured separately as well as simultaneously, and the data were combined to derive the complete product distribution. The rise of product concentrations with time was almost linear over a period of 45 min. Figure 2 shows the rise of C5 carbonyl compounds and pentanols as a function of time to indicate the scatter of individual data points obtained in four separate runs, in which concentrations were measured simultaneously. To make the data compatible, the individual rates were normalized to a common reaction rate corresponding to an H<sub>2</sub>O<sub>2</sub> starting mixing ratio of 120 ppm. Additional runs at constant reaction times were made to improve the precision of the measurements. Table III shows the averaged product distribution pieced together from the results of altogether 25 runs. This distribution provides relative product concentrations in percent of the total observed concentration. The calculations discussed below indicate the formation of other products, such as hydroperoxides, which were not observed and are not included.

With the assumption that the mutual reactions of *n*-pentylperoxy radicals feature similar branching ratios, one may use the observed distribution of the pentanols to estimate relative probabilities for hydrogen abstraction by OH radicals at the three different sites of *n*-pentane. The measured distribution for pentan-1-ol, pentan-2-ol, and pentan-3-ol:  $9.1 \pm 0.7\%$ ,  $56.1 \pm 1.8\%$ , and  $34.8 \pm 1.3\%$ , indicates relative probabilities of approximately  $q_1 = 0.09$ ,  $q_2 = 0.56$ , and  $q_3 = 0.35$ , for the formation of pentan-1-peroxy, pentan-2-peroxy, and pentan-3-peroxy, respectively, and these values were initially used in the calculations. Other parameters were taken from our previous study:  $\alpha_{11} = 0.42$ ,  $\alpha_{22} = 0.46$ ,  $\alpha_{33} = 0.40$ ,  ${}^1 k_{\text{isom}} = 4.0 \times 10^5$  s<sup>-1</sup>,  ${}^2 k_{\text{isom}} = 1.1 \times 10^5$  s<sup>-1</sup>,  ${}^2 k_{\text{dec}} = 8.4 \times 10^3$  s<sup>-1</sup>,  ${}^3 k_{\text{dec}} = 2.6 \times 10^4$  s<sup>-1</sup> (see

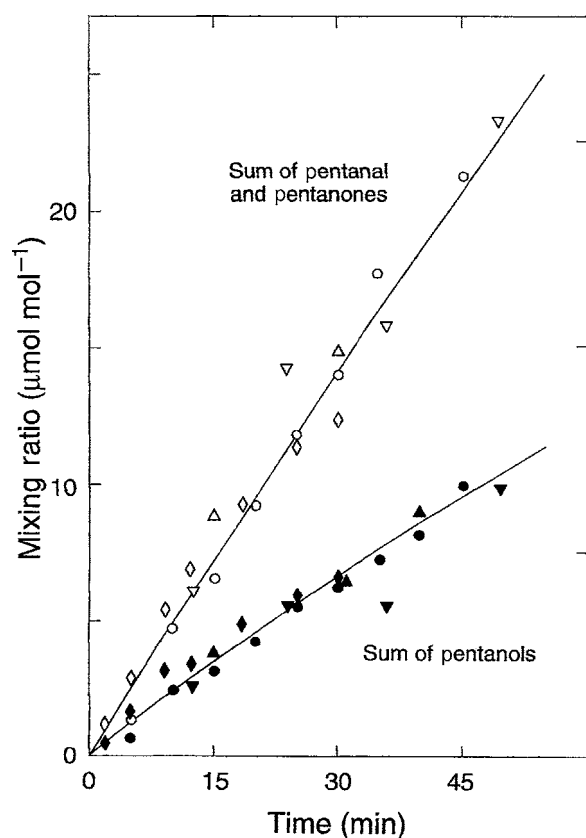


**Figure 2** Rise with time of the sum of pentanols and the sum of pentanones and pentanal during the oxidation of *n*-pentane (for the individual contributions of compounds, see Table III). Data from three runs (circles, triangles, and diamonds) are normalized to a common total reaction rate corresponding to an initial  $\text{H}_2\text{O}_2$  mixing ratio of 120 ppm. The solid lines are calculated with parameters providing an optimal approximation of the observed product distribution (penultimate column of Table III).

Table II). The low yield of diols found in that study [9] had suggested that branching ratios associated with reactions of hydroxy-pentylperoxy radicals are greater than those for alkylperoxy radicals in general, approximately  $\alpha_{6j} \approx \alpha_{7j} \approx 0.8$  (where  $j = 1-7$ ), and this value was used. All other branching ratios were initially set to 0.5, and it was assumed that  $y_{ki} = z_{ki} = 0.5$  for the cross-combination reactions (for definitions, see Table I). The decomposition of pentan-1-oxyl was neglected. The rate coefficient theoretically estimated for the split-off of formaldehyde is small compared to that for isomerization [12], and the butyl radical formed simultaneously should be partly oxidized to butanal, which was not identified as a product. The two hydroxy-pentoxyl radicals derived from the corresponding peroxy precursors (numbers 6 and 7 in Fig. 1) were assumed to isomerize rapidly

as shown in Table I (with  ${}^6k_{\text{isom}} \approx {}^7k_{\text{isom}} \geq 2 \times 10^6 \text{ s}^{-1}$ ); decomposition reactions should be much slower and were ignored. The ultimate products are stable hydroxy-carbonyl compounds: 4-hydroxy-pentanal and 1-hydroxy-pentan-4-one, respectively.

The product distribution calculated for 30 min reaction time is presented in column (a) of Table III. It is in surprisingly good agreement with the experimental data shown in the preceding column. Obvious differences are the higher yields of the pentanols, the nearly equal yield of pentanal and pentan-1-ol, which is in contrast to the observed ratio  $[\text{pentanal}]/[\text{pentan-1-ol}] = 1.97 \pm 0.91$ , and the higher relative yield of the sum of pentanal and pentan-1-ol compared to the observed yield. This suggests a need for raising some of the branching ratios and lowering the probability of pentan-1-peroxy formation. The calculations revealed that the dominant reactions in the system are the self-reactions of pentan-2-peroxy and pentan-3-peroxy radicals, their mutual interaction, and reactions with the primary 4-hydroxy-pentan-1-peroxy radical that derives from the isomerization of pentan-2-oxyl. Pentan-1-peroxy radicals, in contrast, react with most of the other peroxy radicals at nearly equal rates, but these are less important because of the lower probability at which pentan-1-peroxy radicals are generated. Column (b) in Table III presents the product distribution obtained after the following changes in the parameters:  $q_1 = 0.07$ ,  $q_2 = 0.58$ , and  $q_3 = 0.35$ ;  $\alpha_{11} = \alpha_{22} = 0.56$ ,  $\alpha_{33} = 0.50$ . These changes improve the distribution between pentanols and pentanones, but not that between pentan-1-ol and pentanal. A better representation of the latter can be achieved by adjusting the ratio of pentan-1-ol to pentanal formed in the cross-combination reactions of pentan-1-peroxy radicals with secondary peroxy radicals in the system: pentan-2-peroxy, pentan-3-peroxy, and 1-hydroxy pentan-4-peroxy (numbers 2, 3, and 6 in Fig. 1). This required changes in the parameters  $y_{1i}$  and  $z_{1i}$  that determine the distribution of carbonyl compounds and alcohols resulting as products from pentan-1-peroxy radical cross reactions (see Table I). Subsequent calculations used  $y_{12} = y_{13} = y_{16} = 0.65$ ,  $z_{12} = z_{13} = z_{16} = 0.35$ , whereas  $y_{ki} = z_{ki} = 0.5$  was retained for all other cross-combination reactions. Finally, the parameters for the initial distribution of pentylperoxy radicals were slightly readjusted:  $q_1 = 0.074$ ,  $q_2 = 0.58$ , and  $q_3 = 0.346$ ; the branching ratios for the cross-combination reactions were raised from 0.5 to 0.56, whereas the branching ratios for the self-reactions of pentyl peroxy radicals were set at  $\alpha_{11} = \alpha_{22} = 0.56$ , and  $\alpha_{33} = 0.50$ . The final product distribution, which is shown in column (c) of Table III,

**Table III** Oxidation of *n*-Pentane: Observed and Calculated Product Distributions after 30 min Reaction Time

|                             | Observed                  | Calculated <sup>d</sup> |                    |                    |                   | Observed                 |
|-----------------------------|---------------------------|-------------------------|--------------------|--------------------|-------------------|--------------------------|
|                             | (%)                       | a (%)                   | b (%)              | c (%)              | d <sup>b</sup>    | e <sup>b</sup>           |
| Pentan-1-ol                 | 1.59 ± 0.13               | 2.70                    | 2.00               | 1.58               | 0.56              | 0.56 ± 0.05              |
| Pentan-2-ol                 | 9.79 ± 0.31               | 12.17                   | 10.77              | 10.36              | 3.68              | 3.47 ± 0.11              |
| Pentan-3-ol                 | 6.07 ± 0.23               | 7.57                    | 6.56               | 6.19               | 2.20              | 2.16 ± 0.08              |
| Pentanal                    | 3.01 ± 1.20               | 3.40                    | 2.59               | 3.00               | 1.07              | 1.07 ± 0.43              |
| Pentan-2-one                | 19.18 ± 3.61              | 20.19                   | 20.19              | 19.08              | 6.76              | 6.83 ± 1.28              |
| Pentan-3-one                | 18.48 ± 3.45              | 18.18                   | 18.32              | 18.14              | 6.44              | 6.58 ± 1.23              |
| Ethanal                     | 8.69 ± 1.89               | 6.70                    | 7.51               | 7.81               | 2.78              | 3.09 ± 0.67              |
| Propanal                    | 7.47 ± 1.95               | 7.90                    | 8.81               | 8.97               | 3.24              | 2.66 ± 0.69              |
| Ethanol                     | 1.47 ± 0.18               | 1.41                    | 1.54               | 1.45               | 0.51              | 0.52 ± 0.06              |
| Propan-1-ol                 | 1.09 ± 0.39               | 0.35                    | 0.40               | 0.36               | 0.13              | 0.38 ± 0.14              |
| Isomer. Prod.               | 23.16 ± 4.29 <sup>c</sup> | 19.42 <sup>d</sup>      | 21.39 <sup>d</sup> | 23.06 <sup>d</sup> | 8.21 <sup>d</sup> | 8.24 ± 1.53 <sup>c</sup> |
| 1,4 Pentandiol              | –                         | –                       | –                  | –                  | 0.91              | n. d.                    |
| Hydroperoxides <sup>e</sup> | –                         | –                       | –                  | –                  | 17.34             | n. d.                    |

<sup>a</sup> See text for conditions assumed in the calculations. Columns a, b, and c give percentage distributions; results in column d (in  $\mu\text{mol mol}^{-1}$ ) correspond to those in column c.

<sup>b</sup> Product distribution in units of  $\mu\text{mol mol}^{-1}$ ; the experimental data are adjusted to fit the same initial  $\text{H}_2\text{O}_2$  concentration as in the calculations ( $120 \mu\text{mol mol}^{-1}$ ); n. d. = not determined.

<sup>c</sup> Contribution of the unidentified peak seen on the CP-Sil column that is attributed to an isomerization product.

<sup>d</sup> Calculated as sum of 4-hydroxy-pentanal and 1-hydroxy-pentan-4-one.

<sup>e</sup> Pentyl-2-hydroperoxide contributes 56% and pentyl-3-hydroperoxide 35% to the total.

demonstrates that observed and calculated product distributions can be brought into reasonable agreement simply by adjusting probabilities of pentylperoxyl radical formation and branching ratios of pentylperoxyl reactions. It was not necessary to change rate coefficients of cross-combination reactions.

The last two columns of Table III compare calculated and experimental product concentrations. Hydroperoxides contribute 32% to the sum of all products, with 90% being due to the two secondary pentylhydroperoxides; 1,4 pentan-diol contributes only 1.7%. Neither of these has been detected by the analytical procedures employed.

It should be reiterated that the amounts of isomerization products listed in Table III as having been observed refer to a gas chromatographic peak occurring at a retention time typical of C5 hydroxy-carbonyl compounds that were not specified, whereas the calculations refer to the sum of 4-hydroxy-pentanal and 1-hydroxy-pentan-4-one. Thus, the agreement between observation and calculation refers only to the extent of isomerization, not to the individual products that are involved.

### Isopentane

Major products appearing in the gas chromatograms were acetone, acetaldehyde, 2-methyl-butan-2-ol, and 2-methyl-butan-2-hydroperoxide. Additional, less abundant products were 2-methyl-3-butanone, 2-

methyl-butan-3-ol, and ethanol. Also observed were 2-methyl-butanal and 3-methyl-butanal, but these could not be quantified because their peaks overlapped with the much larger peak of 2-methyl-butan-3-one. Accordingly, their abundances could only be estimated. Propan-2-ol, which is an expected product, could not be observed because the corresponding peak was hidden underneath the much larger peak of isopentane on both gas chromatographic columns used. Identification of 2-methyl-butan-2-hydroperoxide as a product was confirmed in separate experiments by adding CO to the reaction mixture, so that some of the hydroxyl radicals were converted to  $\text{HO}_2$ , which subsequently by reacting with 2-methyl-butan-2-peroxyl increased the production of the tertiary hydroperoxide. This procedure has been found useful in our previous study of the oxidation of 2,3-methyl-butane [15]. Figure 3 shows the rise of the four major products as a function of time to indicate the scatter of individual data points. Again, the rates of individual runs were normalized to a common reaction rate corresponding to an  $\text{H}_2\text{O}_2$  starting mixture of 120 ppm. Table IV shows the percentage distribution of the observed products derived from seven different runs. This distribution does not include 2-methyl-butanal and 3-methyl-butanal owing to the experimental uncertainties in their quantification, but they are included in the last column of Table IV, which compares normalized average experimental mixing ratios with those derived by calculations.

**Table IV** Oxidation of Isopentane: Observed and Calculated Product Distributions after 30 min Reaction Time

|                               | Observed     | Calculated <sup>a</sup> |       |       |                | Observed       |
|-------------------------------|--------------|-------------------------|-------|-------|----------------|----------------|
|                               | (%)          | a                       | b     | c     | d <sup>b</sup> | e <sup>b</sup> |
| Acetone                       | 26.93 ± 2.21 | 27.92                   | 28.94 | 27.76 | 13.92          | 13.50 ± 1.11   |
| Acetaldehyde                  | 26.06 ± 2.45 | 24.27                   | 26.69 | 26.38 | 13.07          | 13.07 ± 1.22   |
| <i>tert</i> -Hydroperoxide    | 15.37 ± 4.01 | 21.02                   | 15.38 | 15.48 | 7.77           | 7.71 ± 2.01    |
| 2-Methyl butan-2-ol           | 14.65 ± 3.63 | 9.76                    | 15.82 | 14.62 | 7.33           | 7.35 ± 1.82    |
| 2-Methyl butan-3-one          | 10.15 ± 4.01 | 10.31                   | 8.04  | 10.09 | 5.06           | 5.09 ± 2.01    |
| 2-Methyl butan-3-ol           | 3.61 ± 2.42  | 3.31                    | 3.02  | 3.65  | 1.85           | 1.81 ± 1.21    |
| Ethanol                       | 3.21 ± 0.54  | 3.40                    | 2.10  | 2.00  | 0.98           | 1.62 ± 0.27    |
| Propan-2-ol                   | —            | —                       | —     | —     | 0.55           | n. d           |
| 2-Methyl-butanal              | —            | —                       | —     | —     | 1.89           | 1.55 ± 0.63    |
| 3-Methyl-butanal              | —            | —                       | —     | —     | 0.87           | 1.25 ± 0.63    |
| 2-Methyl butan-1-ol           | —            | —                       | —     | —     | 0.43           | n. d           |
| 3-Methyl butan-1-ol           | —            | —                       | —     | —     | 0.21           | n. d           |
| Isomer. Products <sup>c</sup> | —            | —                       | —     | —     | 1.93           | n. d           |
| 2-Methyl butan-1,4 diol       | —            | —                       | —     | —     | 0.10           | n. d           |
| Hydroperoxides <sup>d</sup>   | —            | —                       | —     | —     | 3.52           | n. d           |

<sup>a</sup> See text for conditions assumed in the calculations. Columns "a," "b," and "c" give percentage distributions; results in column "d" (in  $\mu\text{mol mol}^{-1}$ ) correspond to those in column "c."

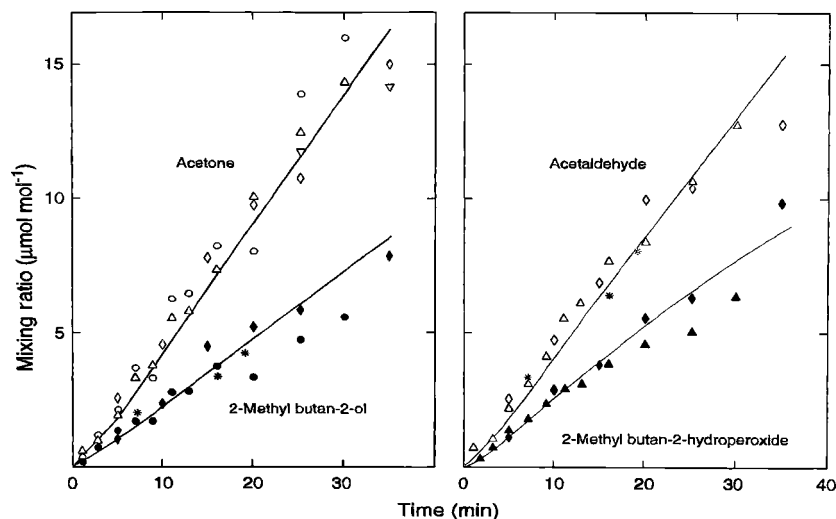
<sup>b</sup> Product distribution in units of  $\mu\text{mol mol}^{-1}$ ; the experimental data are adjusted to fit the same initial  $\text{H}_2\text{O}_2$  concentration as in the calculations ( $120 \mu\text{mol mol}^{-1}$ ); n. d. = not determined.

<sup>c</sup> Sum of 4-hydroxy 2-methyl-butanal and 4-hydroxy 3-methyl-butanal.

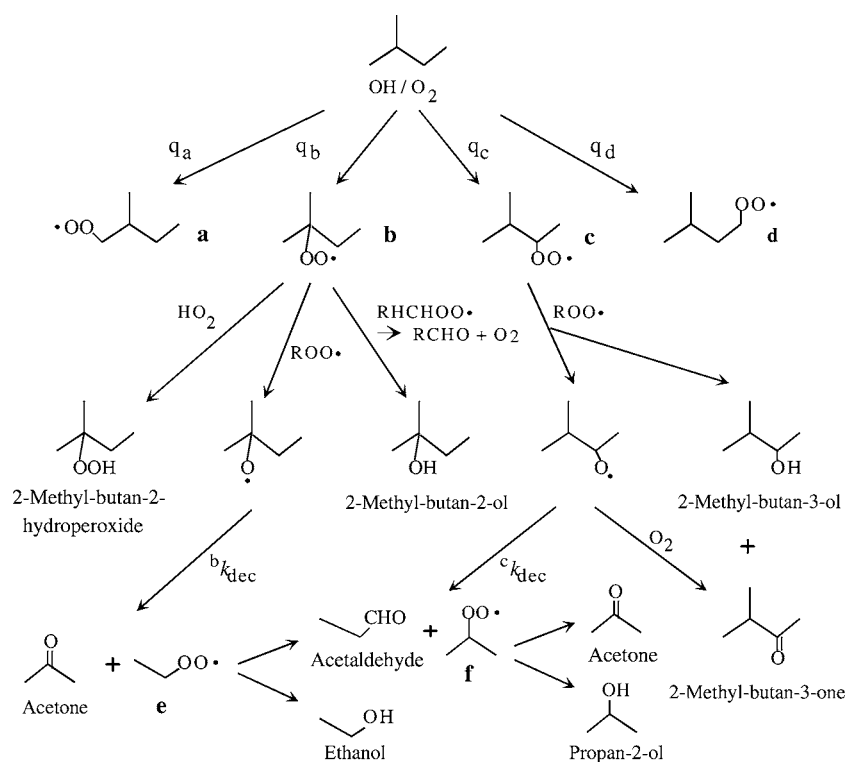
<sup>d</sup> Other than 2-methyl butan-2-hydroperoxide; 2-methyl butan-3-hydroperoxide is the second major contributor.

Figure 4 presents an abbreviated scheme for the oxidation of isopentane, which forms the basis for computer simulations. Only the major oxidation pathways following production of the primary peroxy radicals **b** and **c** are shown. The other two primary radicals **a** and **d**, which are formed by hydrogen abstraction from the methyl groups of isopentane and

addition of oxygen, are assumed to react in analogy to pentan-1-peroxy, whose reactions are shown in Table I. The total oxidation scheme involves altogether eight peroxy radicals. In addition to the six radicals **a-f** shown in Fig. 4, one must consider 1-hydroxy-2-methyl-butan-4-peroxy and 1-hydroxy-3-methyl-butan-4-peroxy arising from isomerization



**Figure 3** Rise with time of the major products: acetone, acetaldehyde, 2-methyl butan-2-ol, and 2-methyl butan-2-hydroperoxide during the oxidation of isopentane. Data from different runs are normalized to a common total reaction rate corresponding to an initial  $\text{H}_2\text{O}_2$  mixing ratio of 120 ppm. Data obtained from the same runs are identified by circles, triangles, diamonds, and asterisks, respectively. The solid lines result from calculations based on an optimal choice of parameters (penultimate column of Table IV).



**Figure 4** Oxidation mechanism of isopentane. Only reaction pathways evolving from tertiary 2-methyl butan-2-peroxyl and secondary 2-methyl butan-3-peroxyl are shown. Reaction pathways for the other two peroxyl radicals initially formed (**a** and **d**) are treated like butan-1-peroxyl (see text for details).

of the corresponding 2-methyl-butan-1-oxyl and 3-methyl-butan-1-oxyl precursors. The first of these was assumed to isomerize at the same rate as butan-1-oxyl, which has been well studied, experimentally [19–22] as well as theoretically [14]. In this case, the isomerization rate coefficient has an average value of  $1.6 \times 10^5 \text{ s}^{-1}$ . Isomerization of 3-methyl-butan-1-oxyl should be twice as rapid because two methyl groups are available for internal hydrogen abstraction. Accordingly, rate coefficients of  ${}^a k_{\text{isom}} = 1.6 \times 10^5 \text{ s}^{-1}$  and  ${}^d k_{\text{isom}} = 3.2 \times 10^5 \text{ s}^{-1}$ , respectively, were applied for the isomerization of these radicals. The calculations show, however, that reactions and products within the two branches starting from the radicals **a** and **d** in Fig. 4 make only a minor contribution to the overall mechanism.

The reaction sequences shown in Fig. 4 involve the decomposition of 2-methyl-butan-2-oxyl and 2-methyl-butan-3-oxyl. For the first process, which leads to acetone and an ethyl radical, Méreau et al. [13] have calculated a decomposition constant  ${}^b k_{\text{dec}} = 9.4 \times 10^5 \text{ s}^{-1}$ . Batt et al. [23] had earlier reported experimental data obtained at elevated temperatures that when extrapolated to 298 K lead to  $1.6 \times 10^4 \text{ s}^{-1}$ . Both values are large enough to preclude the interference by

conceivable competing reactions. According to Batt et al. [23], decomposition to form butan-2-one and a methyl radical is negligible in comparison to acetone and ethyl as products. Indeed, we have not observed butane-2-one among the products. The rate coefficient for the decomposition of 2-methyl-butan-3-oxyl has not yet been determined, but we can safely assume that its value is similar to, or even larger than, that for butan-2-oxyl, which has been repeatedly studied. In this case, the experimental data [10,20,21,24] average to  $2.2 \times 10^4 \text{ s}^{-1}$ , which agrees well with the value derived theoretically [13],  $3.5 \times 10^4 \text{ s}^{-1}$ . The initial decomposition constant adopted in the computer simulations was  ${}^c k_{\text{dec}} = 4.5 \times 10^4 \text{ s}^{-1}$ , but subsequently it was found necessary to raise the value so as to achieve a better representation of acetaldehyde production.

The observed product distribution does not allow to estimate the relative probabilities for hydrogen atom abstraction from isopentane in the same manner as for *n*-pentane, not only because the products resulting from abstraction at the methyl groups were not quantified, but also because acetone and acetaldehyde derive from both of the two precursor radicals **b** and **c**. The formulas of Greiner [4] and Atkinson [5,6] suggest 12.7% or 11.2%,

respectively, for hydrogen abstraction at the three methyl groups combined. We have adopted an intermediate value of 12% in the computer simulations, so that  $q_a = 0.08$  and  $q_d = 0.04$ . Initial values for the probabilities of formation of tertiary and secondary peroxy radicals were derived as follows: The ratio  $q_b/q_c$  is approximately given by the sum of acetone, 2-methyl-butan-2-ol, and 2-methyl-butan-2-hydroperoxide minus the fraction of acetone resulting from decomposition of the 2-methyl-butan-3-oxyl radical, divided by the sum of 2-methyl-butan-3-one and 2-methyl-butan-3-ol, corrected for the fraction of decomposition of 2-methyl-butan-3-oxyl. From the observed product distribution in Table IV, we estimate that  $q_b/q_c \approx (56.95 - 3.61)/(13.76 + 3.61) = 3.07$ ; the additional condition  $q_b + q_c = 0.88$  then leads to  $q_b \approx 0.66$  and  $q_c \approx 0.22$ . These parameters were initially used in the computer simulations.

Column (a) of Table IV presents the product distribution calculated with the parameters discussed above. Comparison with the experimental data shows that the rate of production of 2-methyl-butan-2-hydroperoxide is calculated too high and that of 2-methyl-butan-2-ol is too low. The production of acetaldehyde also is somewhat low. Trial calculations made evident that the rate of the tertiary hydroperoxide production can be lowered only by decreasing the rate coefficient for the reaction between  $\text{HO}_2$  and 2-methyl-butan-2-peroxy (radical **b** in Fig. 4) from  $k_{\text{HO}_2} = 1.5 \times 10^{-11}$ , used initially, to  $k_{\text{HO}_2} = 6.0 \times 10^{-12}$ , and this value was subsequently applied. The rate of formation of 2-methyl-butan-2-ol is primarily determined by the interaction of 2-methyl-butan-2-peroxy with ethyl-peroxy, and to a lesser extent with 2-methyl-butan-3-peroxy (radicals **e** and **c** in Fig. 4). Accordingly, the rate coefficient for the reaction between primary and tertiary peroxy radicals was increased from  $2.0 \times 10^{-15} \text{ cm}^3 \text{ molecule}^{-1} \text{ s}^{-1}$  used initially to  $k_{\text{pt}} = 6.0 \times 10^{-15} \text{ cm}^3 \text{ molecule}^{-1} \text{ s}^{-1}$ . The rate coefficient for the decomposition of the 2-methyl-butan-3-oxyl radical was also increased from the initial value  $4.5 \times 10^4 \text{ s}^{-1}$  to  ${}^c k_{\text{dec}} = 8.5 \times 10^4 \text{ s}^{-1}$ . These changes in the parameters resulted in the product distribution shown in column (b) of Table IV. The production rates of 2-methyl-butan-2-ol and 2-methyl-butan-2-hydroperoxide compare more favorably with the experimental data, and that of acetaldehyde has also improved. However, the rates of formation of 2-methyl-butan-3-one and 2-methyl-butan-3-ol are too low, indicating a need for readjustment of the probabilities for hydrogen abstraction from isopentane. The values  $q_b = 0.60$  and  $q_c = 0.28$  were found to provide a product distribution that compares well with the experimental data. In the final fit, which is shown in Table IV in column (c), the branching ratios associated with reac-

tions of secondary peroxy radicals were raised slightly to  $\alpha_{\text{ss}} = \alpha_{\text{sp}} = 0.55$ . The last two columns in Table IV compare calculated and scaled experimental product mixing ratios after 30 min reaction time. Ethanol is the only product, which is significantly underrepresented in the final calculation. This is caused by the important role of  $\text{CH}_3\text{CH}_2\text{OO}^\bullet$  radicals in the formation of 2-methyl-butan-2-ol by reacting with 2-methyl-butan-2-peroxy. The situation would improve, if 2-methyl-butan-3-peroxy radicals would share in this role. This may be accomplished by setting  $k_{\text{pt}} = 4.0 \times 10^{-15}$  and  $k_{\text{st}} = 4.0 \times 10^{-16} \text{ cm}^3 \text{ molecule}^{-1} \text{ s}^{-1}$ , but in this case the decomposition constant of 2-methyl-butan-3-oxyl would have to be raised to  ${}^c k_{\text{dec}} \approx 1.5 \times 10^5 \text{ s}^{-1}$  in order to obtain a product distribution in harmony with the experimental data.

## DISCUSSION

Three aspects deserve discussion: one is the relative probability of hydrogen abstraction, another deals with the branching ratios associated with the mutual reactions of pentylperoxy radicals, and the third concerns the comparison of observed and calculated product distributions.

### *n*-Pentane

Relative probabilities for hydrogen abstraction at different sites of *n*-pentane were derived from the distribution of the alcohols and from a comparison of calculated product distributions with the experimental data. The former results are, in percent,  $q_1 = 9.1 \pm 0.7$ ,  $q_2 = 56.1 \pm 1.8$ , and  $q_3 = 34.8 \pm 1.3$ , whereas the latter are 7.4, 58.0, and 34.6, respectively. Both correspond rather closely to the probabilities calculated with the algorithm for alkanes proposed by Atkinson [5,6], which gives 9.4%, 55.1%, and 35.5%. This contrasts with results obtained with the formulas developed by Greiner [4], which lead to 10.4%, 59.7%, and 29.9%. It is remarkable that the present observations and the theoretical predictions, which are based on a few selected hydrocarbons that did not include *n*-pentane, provide such a good agreement. In addition, the individual rate coefficients calculated by using the method of Atkinson sum to a total  $k_{\text{OH}} = 3.9 \times 10^{-12} \text{ cm}^3 \text{ molecule}^{-1} \text{ s}^{-1}$ , close to the measured value [1,2]  $4.0 \times 10^{-12}$ , whereas the formulas of Greiner lead to  $3.7 \times 10^{-12} \text{ cm}^3 \text{ molecule}^{-1} \text{ s}^{-1}$ . The Kwok and Atkinson [6] estimation method is based on a much larger data base for reactions of OH with alkanes than the earlier calculation by Greiner [4]. Hence, it is able to take into account the effect of near neighbors and should be more accurate.

The branching ratios for the self-reactions of *n*-pentan-2-peroxyl and *n*-pentan-3-peroxyl radicals that were needed to bring the calculated fractions of pentanols and pentanones into agreement with the experimental data are higher than those that we had derived previously [9], although still within the mutual range of uncertainty. Independent of the model calculations, the product ratios  $R_1 = \text{pentanal/pentan-1-ol}$ ,  $R_2 = \text{pentan-2-one/pentan-2-ol}$ , and  $R_3 = \text{pentan-3-one/pentan-3-ol}$  can be used to estimate effective branching ratios for each of the *n*-pentan-peroxyl isomers involved. The subscripts refer again to the numbers assigned to the radicals shown in Fig. 1. Effective branching ratios can be calculated from  $\bar{\alpha}_i = (R_i - 1)/(R_i - 1 + 2f_i)$ , where  $i = 1, 2$ , or  $3$ , and  $f_i = (1 + {}^i k_{\text{dec}}/k_{\text{O}_2}[\text{O}_2] + {}^i k_{\text{isom}}/k_{\text{O}_2}[\text{O}_2])^{-1}$  refers to decomposition, isomerization and reaction with oxygen of the corresponding *n*-pentoxy radical. The experimental data in Table III provide  $R_1 = 1.97 \pm 0.92$ ,  $R_2 = 1.96 \pm 0.43$ , and  $R_3 = 3.07 \pm 0.68$ . Relative rate coefficients  ${}^i k_{\text{dec}}/k_{\text{O}_2}[\text{O}_2]$  and  ${}^i k_{\text{isom}}/k_{\text{O}_2}[\text{O}_2]$  are taken from our previous determination [9] (see Table II), including the respective error margins. With the above data, one obtains  $\bar{\alpha}_1 = 0.54 \pm 0.35$ ,  $\bar{\alpha}_2 = 0.60 \pm 0.14$ , and  $\bar{\alpha}_3 = 0.59 \pm 0.10$ . These average branching ratios are larger than those that were needed to calculate a product distribution compatible with the experimental data. The difference probably reflects the influence of the fairly large branching ratio adopted in the calculations for reactions of 4-hydroxy-pentan-1-peroxyl and 1-hydroxy-pentan-4-peroxyl radicals.

Table III shows that by using branching ratios in the range 0.50–0.57 the calculated product distribution can be made to agree well with that derived experimentally. Propan-1-ol is the only exception. In this case the observed amount is higher than calculated. As the only source of propanol are reactions of propan-1-peroxyl, generated by the decomposition of *n*-pentan-2-oxyl, the amount of propanol formed depends only on the parameters  $q_2$  and  ${}^2 k_{\text{dec}}$ . Both leave little room for variation. In the case of ethanol, the calculated and observed values coincide. We consider it unlikely that propan-1-peroxyl and ethyl peroxyl would behave much differently. Therefore, the amount of propan-1-ol derived from the experiments must have been overestimated. The data in Table III also indicate a slight mismatch between experiments and calculations for acetaldehyde and propanal, although the experimental scatter is considerable in both cases, and the calculated values are within the experimental error ranges. Decomposition of pentan-2-oxyl and pentan-3-oxyl yields acetaldehyde and propanal in nearly equal amounts, yet the experiments indicate an excess of acetaldehyde. We had

previously noted [9] that the reactions following the generation of pentan-2-peroxyl radicals produce more acetaldehyde than can be accounted for by the decomposition of propan-2-oxyl, and we had suggested that decomposition of the product arising from isomerization of 4-hydroxy pentan-1-oxyl ( ${}^7 k_{\text{isom}}$ ; see Table I) might be responsible for it.

While the calculations seem to predict correctly the total amount of isomerization products, it must again be cautioned that we have not identified these products experimentally. As the major isomerization product derives from pentan-2-oxyl, the agreement between calculated and experimental data confirms the magnitude of the isomerization constant used,  ${}^2 k_{\text{isom}} = 1.1 \times 10^5 \text{ s}^{-1}$ . In our previous study [9] of the decomposition of iodopentanes, the product assigned to isomerization of the pentan-2-oxyl radical appeared to be unstable giving rise to a number of other products. In the present experiments, only one major isomerization product was detected. The low yield of pentan-1-ol is surprising, and our attempt to rationalize it by lowering the fraction of pentan-1-peroxyl radicals entering into the pentan-1-ol forming channel requires further scrutiny.

### Isopentane

It was not possible to derive from the observed product distribution the relative probabilities for hydrogen abstraction at all four sites of isopentane. The probability for H-atom abstraction at the methyl groups was estimated with the formulas presented by Atkinson [5,6] and Greiner [4] as  $\sim 12\%$ . The relative probabilities for the formation of 2-methyl-butan-2-peroxyl and 2-methyl-butan-3-peroxyl were then obtained by comparison of simulated and observed product distributions. This procedure leads to  $q_a = 8.0\%$ ,  $q_b = 60.0\%$ ,  $q_c = 28.0\%$ , and  $q_d = 4.0\%$ . This compares well with probabilities calculated from the algorithm proposed by Atkinson [5,6], which are 7.43%, 60.85%, 28.0%, and 3.72%, respectively, whereas the formulas of Greiner [4] give 8.4%, 63.0%, 24.4%, and 4.2%. As in the case of *n*-pentane, we can calculate the total rate constant by summing the individual rate constants. The algorithm of Atkinson [5,6] gives for isopentane  $k_{\text{OH}} = 3.87 \times 10^{-12} \text{ cm}^3 \text{ molecule}^{-1} \text{ s}^{-1}$ , which is close to the measured value  $3.7 \times 10^{-12}$  [1], whereas the formulas of Greiner [4] lead to  $4.57 \times 10^{-12} \text{ cm}^3 \text{ molecule}^{-1} \text{ s}^{-1}$ . The present results obviously are in better agreement with Atkinson's method of estimating probabilities for hydrogen abstraction than with Greiner's, for both *n*-pentane and isopentane. However, the former method is based on a larger data base and takes into account the effects of nearest neighbors so that it should be more accurate.

The product distribution obtained from the oxidation of isopentane is dominated by acetone and acetaldehyde. The source of both is primarily the decomposition of 2-methylbutan-2-oxyl and the subsequent interaction of ethyl peroxy with 2-methylbutan-2-oxyl, which consumes approximately 56% of the former and 42% of the latter peroxy radical. Approximately 73% of both products, acetone and acetaldehyde, are formed along this pathway. The remainder derives from the decomposition of 2-methylbutan-3-oxyl. The large fraction of 2-methylbutan-2-ol among the products demonstrates the importance of reactions between 2-methylbutan-2-oxyl and the other peroxy radicals, of which  $\text{CH}_3\text{CH}_2\text{OO}^\bullet$  and 2-methylbutan-3-oxyl are dominant. This is in contrast to the case of 2,3-dimethylbutane oxidation studied by us previously [9], where the rate of tertiary alcohol formation was much lower. In order to bring calculated and observed rates of 2-methylbutan-2-ol formation into agreement, it is necessary to increase the rate coefficients of these reactions by at least a factor of two, but this has the consequence that the calculated amount of ethanol is smaller than the observed one. On the other hand, with regard to the reaction between  $\text{HO}_2$  and 2-methylbutan-2-oxyl, the rate coefficient required to bring the calculated fraction of 2-methylbutan-2-hydroperoxide into agreement with the observed one is similar to that applied previously for 2,3-dimethylbutane. Of special interest is the magnitude of the decomposition constant for the 2-methylbutan-3-oxyl radical. The present results suggest a value of  ${}^c k_{\text{dec}} \approx 8.5 \times 10^4 \text{ s}^{-1}$ , although it might be greater. The present results also confirm the conclusions derived by Batt et al. [23], who had found that the 2-methylbutan-2-oxyl radical decomposes overwhelmingly to form acetone and ethyl, whereas the alternative decomposition pathway resulting in butan-2-one and a methyl radical is unimportant in comparison. The fate of the primary peroxy radicals formed by hydrogen abstraction from the methyl groups of isopentane and the alkoxy radicals appearing in the corresponding oxidation chains could not be explored and remains undetermined.

## SUPPLEMENTARY INFORMATION

Computer programs containing the complete reaction mechanisms for the oxidation of *n*-pentane and isopentane are available from the corresponding author.

The experimental part of this study was a contribution to the EUROTRAC project LACTOZ. We thank H.-J. Benkelberg for carrying out a few supplementary experiments.

## BIBLIOGRAPHY

1. Atkinson, R. *J Phys Chem Ref Data* 1997, 26, 215–290.
2. Atkinson, R.; Arey, J. *Chem Rev* 2003, 103, 4605–4638.
3. Orlando, J. J.; Tyndall, G. S.; Wallington, T. J. *Chem Rev* 2003, 103, 4657–4689.
4. Greiner, N. R. *J Chem Phys* 1970, 53, 1070–1976.
5. Atkinson, R. *Int J Chem Kinet* 1987, 19, 799–828.
6. Kwok, E. C. S.; Atkinson, R. *Atmos Environ* 1995, 29, 1685–1696.
7. Dóbbé, S.; Bérces, T.; Márta, F. *Int J Chem Kinet* 1986, 18, 329–344.
8. Atkinson, R.; Kwok, E. S. C.; Arey, J.; Aschman, S. *Faraday Discuss* 1995, 100, 23–37.
9. Heimann, G.; Benkelberg, H. J.; Böge, O.; Warneck, P. *Int J Chem Kinet* 2002, 34, 126–138.
10. Meunier, N.; Doussin, J. F.; Chevallier, E.; Durand-Jolibois, R.; Picquet-Varrault, B.; Carlier, P. *Phys Chem Chem Phys* 2003, 5, 4834–4839.
11. Atkinson, R. *Int J Chem Kinet* 1997, 29, 99–111.
12. Somnitz H.; Zellner, R. *Phys Chem Chem Phys* 2000, 2, 1907–1918; 4319–4325.
13. Méreau, R.; Rayez, M. T.; Caralp, F.; Rayez, J. C. *Phys Chem Chem Phys* 2000, 2, 3765–3772.
14. Méreau, R.; Rayez, M. T.; Caralp, F.; Rayez, J. C. *Phys Chem Chem Phys* 2003, 5, 4828–4833.
15. Heimann, G.; Warneck, P. *J Phys Chem* 1992, 96, 8403–8409.
16. Curtis, A. R.; Sweetenham, W. P. *Facsimile/Checkmat Users Manual; Aere-R-12805, Her Majesty's Stationary Office: London; 1988.*
17. Lightfoot, P. D.; Cox, R. A.; Crowley, J. N.; Destriau, M.; Hayman, G. D.; Jenkin, M. E.; Moortgat, G. K.; Zabel, F. *Atmos Environ* 1992, 26A, 1805–1964.
18. Madronich, S.; Calvert, J. G. *J Geophys Res* 1990, 95, 5697–5715.
19. Carter, W. P. L.; Lloyd, A. C.; Sprung, J. L.; Pitts, J. N., Jr. *Int J Chem Kinet* 1979, 11, 45–101.
20. Cox, R. A.; Patrick, K. F.; Chant, S. A. *Environ Sci Technol* 1981, 15, 587–592.
21. Niki, H.; Maker, P. D.; Savage, C. M.; Breitenbach, L. P. *J Phys Chem* 1981, 85, 2698–2700.
22. Heiss, A.; Sahetchian, K. *Int J Chem Kinet* 1996, 28, 531–544.
23. Batt, L.; Islam, T. S. A.; Rattray, G. N. *Int J Chem Kinet* 1978, 10, 931–943.
24. Libuda, H. G.; Shestakov, O.; Theloke, J.; Zabel, F. *Phys Chem Chem Phys* 2002, 4, 2579–2586.